IJC Heart & Vasculature 33 (2021) 100747

Contents lists available at ScienceDirect

IJC Heart & Vasculature

journal homepage: www.journals.elsevier.com/ijc-heart-and-vasculature

Coronary lipid-rich plaque characteristics in Japanese patients with acute coronary syndrome and stable angina: A near infrared spectroscopy and intravascular ultrasound study

Norihito Takahashi [a], Tomotaka Dohi [a,*], Hirohisa Endo [a], Mitsuhiro Takeuchi [a], Shinichiro Doi [a], Yoshiteru Kato [a], Iwao Okai [a], Hiroshi Iwata [a], Shinya Okazaki [a], Kikuo Isoda [a], Katsumi Miyauchi [a], Tohru Minamino [a,b]

[a] Department of Cardiovascular Biology and Medicine, Juntendo University Graduate School of Medicine, 2-1-1 Hongo, Bunkyo-ku, Tokyo 113-0033, Japan
[b] Japan Agency for Medical Research and Development Core Research for Evolutionary Medical Science and Technology (AMEDCREST), Japan Agency for Medical Research and Development, 1-7-1 Otemachi, Chiyoda-ku, Tokyo, Japan

ARTICLE INFO

Article history:
Received 31 January 2021
Received in revised form 17 February 2021
Accepted 20 February 2021

Keywords:
Vulnerable plaque
NIRS
Intracoronary imaging
Lipid core burden index
LCBI
Asian

ABSTRACT

Background: Asians have a much lower incidence of adverse coronary events than Caucasians. We sought to evaluate the characteristics of coronary lipid-rich plaques (LRP) in Asian patients with acute coronary syndrome (ACS) and stable angina (SA). We also aimed to identify surrogate markers for the extent of LRP.
Methods: We evaluated 207 patients (ACS, n = 75; SA, n = 132) who underwent percutaneous coronary intervention under near infrared spectroscopy intravascular ultrasound (NIRS-IVUS). Plaque characteristics and the extent of LRP [defined as a long segment with a 4-mm maximum lipid-core burden index ($maxLCBI_{4mm}$)] on NIRS in de-novo culprit and non-culprit segments were analyzed.
Results: The ACS culprit lesions had a significantly higher $maxLCBI_{4mm}$ (median [interquartile range (IQR)]: 533 [385–745] vs. 361 [174–527], $p < 0.001$) than the SA culprit lesions. On multivariate logistic analysis, a large LRP (defined as $maxLCBI_{4mm} \geq 400$) was the strongest independent predictor of the ACS culprit segment (odds ratio, 3.87; 95% confidence interval, 1.95–8.02). In non-culprit segments, 19.8% of patients had at least one large LRP without a small lumen. No significant correlation was found between the extent of LRP and systematic biomarkers (hs-CRP, IL-6, TNF-α), whereas the extent of LRP was positively correlated with IVUS plaque burden ($r = 0.24$, $p < 0.001$).
Conclusions: We confirmed that NIRS-IVUS plaque assessment could be useful to differentiate ACS from SA culprit lesions, and that a threshold $maxLCBI_{4mm} \geq 400$ was clinically suitable in Japanese patients. No surrogate maker for a high-risk LRP was found; consequently, direct intravascular evaluation of plaque characteristics remains important.

1. Introduction

The term "vulnerable plaque" was first proposed in the 1980s, and described plaques that were prone to rupture and triggered coronary events [1]. In autopsy studies, vulnerable plaques had a specific phenotype, which was characterized by an increased plaque burden and a large lipid core [2]. Rupture of the lipid-rich plaque (LRP) causes approximately two-thirds of adverse coronary events, including myocardial infarction and death [3]. Near-infrared spectroscopy (NIRS) can detect LRP on the basis of absorption patterns of the near-infrared light by cholesterol molecules [4]. NIRS intravascular ultrasound (NIRS-IVUS) imaging is dual-modality intravascular imaging system which combines NIRS and IVUS, and allows the simultaneous assessment of plaque morphology and information regarding the cholesterol content in the arterial wall. Several studies have reported the ability of NIRS to identify histological features of LRP, with over 90% sensitivity and specificity for the identification of characteristic features sug-

Abbreviations: ACS, acute coronary syndrome; CI, confidence interval; CKD, chronic kidney disease; hs-CRP, high-sensitive C reactive protein; IL-6, interleukin-6; IQR, interquartile range; IVUS, intravascular ultrasound; LCBI, lipid core burden index; LDL-C, low-density lipoprotein cholesterol; LRP, lipid-rich plaque; MDA-LDL, malondialdehyde-modified LDL; MLA, minimum lumen area; NIRS, near infrared spectroscopy; NSTE-ACS, non-ST elevation acute coronary syndrome; OR, odds ratio; PCI, percutaneous coronary intervention; PCSK9, proprotein convertase subtilisin / kexin type 9; SA, stable angina; STEMI, ST-elevation myocardial infarction; TNF-α, tumor necrosis factor-α.

* Corresponding author.
E-mail address: tdohi@juntendo.ac.jp (T. Dohi).

https://doi.org/10.1016/j.ijcha.2021.100747
2352-9067/

gesting LRP [5,6]. Recent clinical studies have demonstrated that LRP detected by NIRS can predict the risk of further major coronary events [7,8]. In these clinical studies using NIRS, the lipid core burden index (LCBI) cutoff value is set to 400, which is based on the relatively small and limited population investigated in America and Sweden [9]. However, the incidence of acute myocardial infarction in the Asian population including Japan is significantly lower than that of the Western population [10]. Therefore, lipid-rich vulnerable plaque characteristics may differ between ethnicities, and the characteristics of LRP in Asians is unclear. In addition, the circulating surrogate biomarkers associated with LRP detected by NIRS assessment is not known.

The aim of this study was to investigate the clinical characteristics of LRP in the Asian population and we also aimed to distinguish the characteristics of an acute coronary syndrome (ACS) culprit lesion and a stable angina pectoris (SA) culprit lesion. Furthermore, we evaluated the association between LCBI and cardiovascular risk factors, lipid profiles, and inflammatory biomarkers, as determined in vivo by NIRS-IVUS imaging in patients undergoing percutaneous coronary intervention (PCI).

2. Material and methods

2.1. Study population

In this prospective, single-center, observational study, we enrolled consecutive patients who underwent successful PCI under NIRS-IVUS guidance at Juntendo University Hospital (Tokyo, Japan) from March 2017 to March 2020. The inclusion criteria were as follows: (1) patients who underwent PCI to treat a de-novo culprit lesion and (2) patients who underwent NIRS-IVUS imaging of the culprit segment and a non-culprit segment within a native coronary artery. The exclusion criteria were as follows: (1) patients who underwent PCI for an in-stent restenosis lesion and (2) patients in whom adequate IVUS images or NIRS analysis could not be obtained.

Demographic data, coronary risk factors, and medication use were collected on admission from our institutional database. ACS was defined as ST-elevation myocardial infarction (STEMI) or non-ST elevation ACS (NSTE-ACS) [11]. Laboratory data were measured at the time of just before undergoing PCI. The doses of high-intensity statin therapy defined in the European Society of Cardiology guidelines and the American College of Cardiology/American Heart Association guideline are not approved in Japan. According to approved doses in Japan, we defined high-intensity statin therapy as use of rosuvastatin dose of 10–20 mg/day, atorvastatin 20 mg/day, or pitavastatin 4 mg/day. Our definition of moderate or low intensity statin therapy included a prescription for rosuvastatin dose of 5 mg/day, atorvastatin 10 mg/day or pitavastatin 2 mg/day, or rosuvastatin dose of 2.5 mg/day, atorvastatin 5 mg/day or pitavastatin 1 mg/day, respectively.

This study was approved by the Juntendo University Ethnic Committee and was performed in accordance with the Declaration of Helsinki. All participants provided written informed consent.

2.2. NIRS-IVUS image acquisition and analysis

In all study participants, the culprit plaque lesion was imaged pre-intervention by NIRS-IVUS pullback. Combined NIRS and grayscale IVUS image acquisition was performed using the NIRS-IVUS system (TVC Imaging System, Infraredx, Massachusetts, USA or Makoto Imaging System, Infraredx, Massachusetts, USA). Before imaging, 0.1–0.2 mg of intracoronary nitroglycerin was administered. The NIRS-IVUS catheter was inserted distal to the culprit lesion and pulled back at a rate of 0.5 mm/s to the ostium of the coronary artery or guiding catheter. If the NIRS-IVUS catheter could not cross the target lesion, pre-dilatation (using a balloon of 2.0 mm or less) was allowed. All measurements were taken at the end of this study.

All culprit and non-culprit segments in the culprit vessel were analyzed for quantitative and qualitative assessment by IVUS, and the $maxLCBI_{4mm}$ and lesion segment LCBI was assessed by NIRS. A culprit lesion segment was defined as the lesion that was stented by comparing pre- and post-PCI IVUS images. A non-culprit lesion segment was defined as the segment that was proximal or distal to the culprit segment in the culprit vessel. Non-culprit lesions less than 4 mm length were excluded. When the NIRS-IVUS pullback was performed, the pre-stent image was selected for the culprit segment analysis, and the post-stent pullback image was selected for the non-culprit segment analysis. Quantitative and qualitative IVUS analyses were performed according to the criteria of American College of Cardiology Clinical Expert Consensus Document on Standards for Acquisition, Measurement and Reporting of Intravascular Ultrasound Studies and Clinical expert consensus document on standards for measurements and assessment of intravascular ultrasound from the Japanese Association of Cardiovascular Intervention and Therapeutics [12,13].

NIRS data were analyzed to provide a quantitative estimate of the amount of LRP within both the culprit and non-culprit lesion segments. Raw NIRS data were processed by an NIRS algorithm developed using histological data as the standard for LRP detection [4,14]. LCBI is calculated as fraction of pixels with the probability of LRP > 0.6 divided by all pixels with sufficient spectroscopic information, within the region of interest, multiplied by 1000 [14]. $MaxLCBI_{4mm}$ was defined as the maximum LCBI within any 4-mm long segment and lesion-LCBI was defined as the total LCBI throughout each entire segment. In this study, non-culprit high-risk LRP was defined as LRP having a $maxLCBI_{4mm} \geq 400$ [9,15]. A representative case is shown in Fig. 1.

2.3. Statistical analysis

All data were analyzed using JMP version 12.0 (SAS Institute, Inc., NC, USA). Continuous variables are represented as mean (SD) or median [interquartile range]. Categorical data are presented as numbers and ratios (%). Paired data were compared using the Student's *t*-test or the Kruskal–Wallis test. Pearson correlation coefficient and scatter plots were used for continuous variables. Receiver operating characteristic curves were used to determine the cut-off values of $maxLCBI_{4mm}$ to distinguish the ACS culprit lesion with a SA culprit lesion. Multivariate logistic regression analysis controlling for potential confounders was used to calculate the odds ratio (OR) of the ACS culprit lesion such as age, sex, body mass index, hypertension, diabetes, chronic kidney disease (CKD), and plaque burden at the minimum lumen area (MLA). In addition, univariate linear regression analysis was performed to detect the independent effect of the extent of LRP in the culprit lesion. To investigate predictors of high-risk LRP in non-culprit segments, multivariate logistic regression analysis was performed. A p-value of <0.05 was considered to be statistically significant.

3. Results

3.1. Study population and baseline clinical characteristics

Between March 2017 and March 2020, NIRS-IVUS imaging was performed in 251 patients. Of these, a total of 43 patients were excluded because 12 patients had a black chemogram on NIRS examination and 31 patients had an in-stent restenosis lesion.

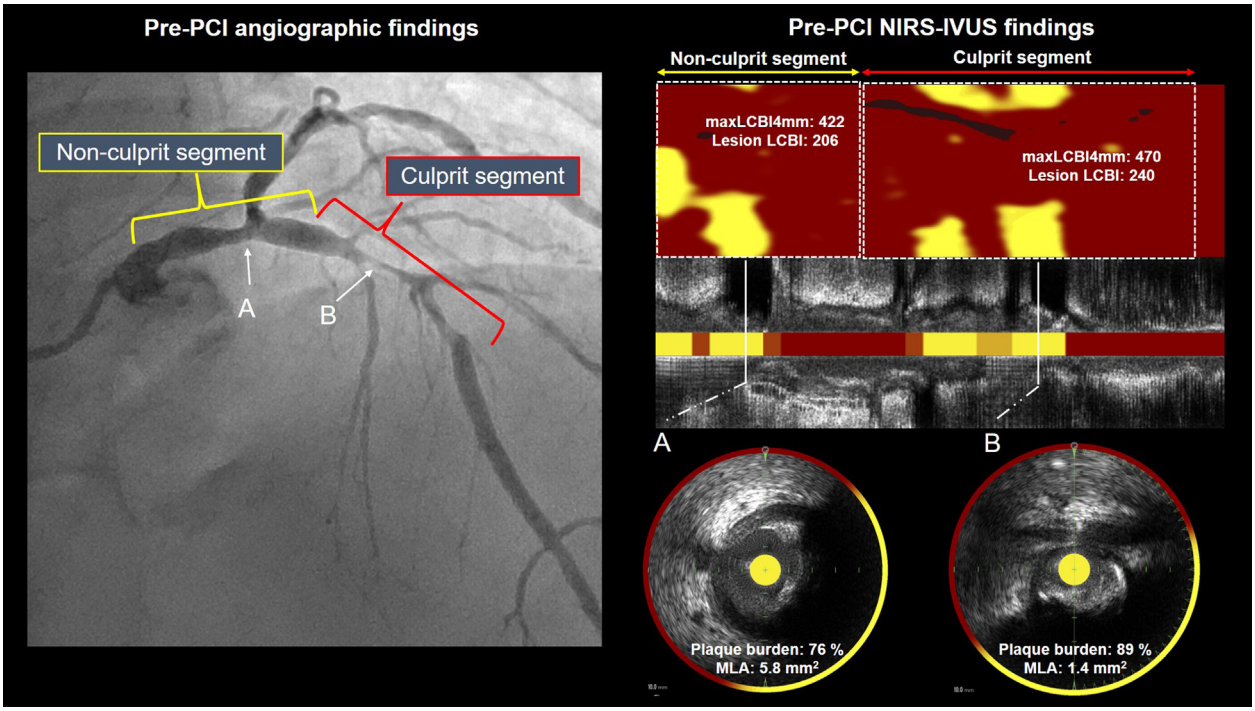

Fig. 1. A representative case of NIRS-IVUS-detected LRP in a culprit lesion and non-culprit lesion. The findings of a 72-year-old man with unstable angina pectoris are shown. On the coronary angiogram, severe coronary stenosis was detected at the LAD proximal portion (B), and mild coronary stenosis was observed at LMT distal portion (A). A Culprit segment was defined as the segment that was stented by comparing pre- and post-PCI IVUS. A non-culprit segment was defined as the segment proximal to that of the culprit segment. Red brackets indicate the culprit segment, and yellow brackets indicate the non-culprit segment. On IVUS examination, an attenuated plaque was observed in the culprit segment and non-culprit segment (PB 76%, MLA 5.8 mm^2 (A), PB 89%, MLA 1.4 mm^2 (B), respectively). NIRS chemogram demonstrated an LRP ($maxLCBI_{4mm}$ 470) at the culprit segment and ($maxLCBI_{4mm}$ 422) the non-culprit segment. PCI, percutaneous coronary intervention; NIRS-IVUS, near infrared spectroscopy and intravascular ultrasound; LCBI, lipid core burden index; PB, plaque burden; MLA, minimum lumen area; LRP, lipid rich plaque; LAD, left descending artery; LMT, left main trunk artery. (For interpretation of the references to colour in this figure legend, the reader is referred to the web version of this article.)

Finally, PCI culprit and non-culprit lesion segment analysis was performed in 207 patients in this study.

Table 1 describes the baseline characteristics of the ACS and SA patients. The mean age was 65.0 (11.2) years old, 82.6% of patients were male, and 36.2% presented with ACS. There were no significant differences in the prevalence of hypertension, dyslipidemia, diabetes, CKD, and multivessel disease between the ACS and SA groups. Patients with ACS had higher levels of low-density lipoprotein cholesterol (LDL-C), malondialdehyde-modified LDL (MDA-LDL), high sensitive C reactive protein (hs-CRP), and interleukin-6 (IL-6) ($p < 0.001$, respectively). Patients with ACS were more likely to be taking statins than with SA (p = 0.025).

3.2. NIRS and IVUS findings in PCI culprit lesions

Overall, 239 PCI culprit lesions were analyzed. IVUS and NIRS findings at the lesion level are summarized in Table 2. In the culprit lesion segments, the median total lesion length, MLA, and plaque burden at the MLA were 23.4 [17.7–31.0] mm, 2.2 [1.7–2.6] mm^2, and 81 [76–86] %, respectively. Total lesion length (25.3 [18.0–32.9] mm vs. 23.0 [17.3–29.9] mm, $p = 0.14$) and MLA (2.1 [1.5–2.6] mm^2 vs. 2.2 [1.7–2.6] mm^2, $p = 0.48$) were similar between the ACS and SA culprit lesions. However, the ACS culprit lesions had a significantly larger plaque burden at the MLA than the SA culprit lesion segment (84 [78–88] % vs. 81 [75–84] %, $p = 0.002$).

In the overall qualitative assessment of culprit lesions, 43.2% and 10.0% of the plaques were described as soft and calcified plaques, respectively. ACS culprit lesions had significantly higher soft plaques and a greater maximum attenuation angle (60.4% vs. 34.3%, $p < 0.001$; 200 [140–278] degrees vs. 120 [0–190] degrees, $p < 0.001$, respectively) compared to SA culprit lesions. NIRS findings showed that the $maxLCBI_{4mm}$ was significantly higher in the ACS culprit lesions than in the SA culprit lesions (533 [385 – 745] vs. 361 [174–527], $p < 0.001$).

Receiver-operating characteristic analysis showed that the NIRS $maxLCBI_{4mm}$ could distinguish the ACS culprit segment from the SA culprit segment, with a sensitivity of 73% and a specificity of 69% (c-statistic = 0.69; $p < 0.001$, cut-off value of max $LCBI_{4mm}$ = 408) (Fig. 2). A plaque burden at the MLA by IVUS could predict lesions with an $maxLCBI_{4mm} \geq 400$, with a sensitivity of 73% and a specificity of 68% (c-statistic = 0.63; $p = 0.001$, cut-off value of plaque burden = 82%).

3.3. NIRS and IVUS findings in PCI non-culprit segments

Overall, 202 PCI non-culprit lesions were analyzed. In the non-culprit segments, 101 (51.5%) segments with a plaque burden at the MLA of over 50% were observed, and 23 (11.7%) segments of with a plaque burden of over 70% were observed. The prevalence of non-culprit segments with LRP, defined as $maxLCBI_{4mm} \geq 400$, was 19.8% without a small lumen (MLA 4.9 [3.4–7.3] mm^2), and with a high plaque burden (plaque burden 61 [56–74] %). In contrast to the culprit lesion, there was no significant difference in the $maxLCBI_{4mm}$, and other qualitive and quantitative IVUS assessments such as the MLA, plaque burden at the MLA, and maximum attenuation angle $\geq 180°$between the ACS and SA non-culprit segments (Table 2).

3.4. Association between LCBI and cardiovascular risk factors, lipid profiles, and inflammatory biomarkers

Pearson correlation coefficient was calculated to ascertain the relationship between the extent of LRP by NIRS $maxLCBI_{4mm}$ and

Table 1
Baseline characteristics of the study population.

	Overall patients (N = 207)	Patients with ACS (N = 75)	Patients with SA (N = 132)	*p*
Age, mean (SD) (years)	65.0 (11.2)	65.9 (12.1)	64.5 (10.6)	0.43
Male, n (%)	171 (82.6)	66 (88.0)	105 (79.5)	0.11
BMI, mean (SD) (kg/m^2)	25.0 (3.8)	24.4 (3.3)	25.4 (4.1)	0.05
Hypertension, n (%)	136 (65.7)	47 (62.6)	89 (67.4)	0.48
Dyslipidemia, n (%)	164 (79.2)	54 (72.0)	110 (83.3)	0.05
Diabetes mellitus, n (%)	88 (42.5)	27 (36.0)	61 (46.2)	0.15
Chronic kidney disease, n (%)	50 (24.1)	22 (29.3)	28 (21.2)	0.19
Current smoking, n (%)	99 (48.5)	35 (48.6)	64 (48.4)	0.98
Family history of CAD, n (%)	45 (22.7)	31 (24.4)	14 (19.7)	0.44
Clinical presentation				<0.001
STEMI, n (%)	40 (19.3)	40 (53.3)	N/A	
NSTE-ACS, n (%)	35 (16.9)	35 (46.6)	N/A	
Stable angina, n (%)	132 (63.7)	N/A	132 (100.0)	
Multivessel disease, n (%)	105 (51.2)	40 (53.3)	65 (50.0)	0.64
Medication				
Statin, n (%)	97 (46.8)	27 (36.4)	70 (52.6)	0.025
High intensity dose, n (%)	12 (5.7)	2 (2.7)	10 (7.5)	
Moderate intensity dose, n (%)	42 (20.2)	13 (17.5)	29 (21.8)	
Low intensity dose, n (%)	43 (20.7)	12 (16.2)	31 (23.3)	
Glucose-lowering drugs, n (%)	67 (32.3)	20 (26.6)	47 (35.6)	0.18
Baseline laboratory findings				
eGFR, median [IQR] (ml/min/m^2)	73.1 [60.4, 85.0]	73.4 [58.3, 85.0]	72.4 [62.6, 84.5]	0.96
HbA1c, median [IQR] (%)	6.1 [5.8, 6.8]	6.2 [5.7, 6.7]	6.1 [5.8, 6.8]	0.59
TG, median [IQR] (mg/dL)	113 [80, 162]	102 [69, 154]	114 [83, 172]	0.14
HDL-C, median [IQR] (mg/dL)	46 [38, 53]	47 [37, 54]	45 [38, 53]	0.70
LDL-C, median [IQR] (mg/dL)	87 [71, 110]	110 [85, 126]	80 [68, 96]	<0.001
Lp (a), median [IQR] (mg/dL)	15 [7, 33]	16 [7,28]	14 [7, 36]	0.70
MDA-LDL, median [IQR] (U/L)	112 [142, 90]	133 [100, 174]	102 [83, 128]	<0.001
Non-HDL, median [IQR] (mg/dL)	113 [95, 133]	107 [94, 124]	134 [108, 158]	<0.001
LDL-C / Apo B, median [IQR]	1.08 [0.98, 1.18]	1.07 [0.97, 1.16]	1.15 [1.06, 1.35]	<0.001
hs-CRP, median [IQR] (mg/L)	0.6 [0.3, 1.9]	5.3 [0.7, 15.9]	0.5 [0.3, 1.4]	<0.001
TNF-α, median [IQR] (pg/mL)	0.51 [0.36, 0.70]	0.52 [0.43, 0.69]	0.49 [0.32, 0.72]	0.31
IL-6, median [IQR] (pg/mL)	2.4 [1.4, 4.7]	1.7 [1.2, 2.9]	3.2 [2.1, 6.9]	<0.001

Values are presented as mean (SD) or median [interquartile range].
ACS, acute coronary syndrome; SA, stable angina pectoris; BMI, body mass index; CKD, chronic kidney disease; CAD, coronary artery disease; LVEF, left ventricular ejection fraction; TG, triglyceride; HDL-C, high-density lipoprotein-cholesterol; LDL-C, low-density lipoprotein-cholesterol; Lp(a), lipoprotein (a); MDA-LDL, malondialdehyde-modified LDL; Apo B, apolipoprotein B; TNF-α, tumor necrosis factor α; IL-6, interleukin-6; hs-CRP, high sensitive C-reactive protein; eGFR, estimated glomerular filtration rate.

clinical biomarkers as systemic risk factors. No significant correlation was found in the study population between the extent LRP and lipid profiles such as LDL-C (r = 0.05, p = 0.52), log Lp(a) (r = 0.06, p = 0.35), and MDA-LDL (r = 0.07, p = 0.28). Among patients with SA, log hs-CRP levels showed a weak correlation with the extent of LRP (r = 0.30, p < 0.001). In patients with diabetes, MDA-LDL levels showed a weak correlation with the extent of LRP (r = 0.23, p = 0.022).

During lesion level analysis, a linear regression model showed no significant correlation between the extent of LRP and cardiovascular risk factors, including HT (coefficient −5.1, 95% confidence interval (CI) −38.2–28.0, p = 0.76), diabetes (coefficient 14.2, 95% CI −17.6–46.0, p = 0.37), and CKD (coefficient 8.3, 95%CI −28.6–45.2, p = 0.65), whereas the plaque burden at the MLA and the maximum attenuation angle showed a significantly linear correlation with the extent of LRP (coefficient 82.3, 95%CI 36.6–127.9, p < 0.001; coefficient 13.0, 95%CI 10.7–15.4, p < 0.001, respectively).

3.5. Independent predictors of ACS culprit lesion

The univariate logistic regression analysis showed that the presence of maxLCBI$_{4mm}$ ≥ 400 (odds ratio (OR), 3.76; 95%CI, 2.12–6.38; p < 0.001) and plaque burden at the MLA (OR 1.88, 95%CI 1.22–3.01, p < 0.001) was significantly associated with ACS culprit lesions. The presence of diabetes (OR 0.59, 95% CI 0.34–1.03, p = 0.06) and CKD (OR 1.55, 95% CI, p = 0.15) tended to be associated with ACS culprit lesions. After adjustment for classical coronary risk factors and plaque burden at the MLA, maxLCBI$_{4mm}$ ≥ 400 was an independent predictor of the ACS culprit segment (adjusted OR, 3.87; 95%CI, 1.95–8.02; p < 0.001) (Table 3).

3.6. Independent predictors of non-culprit high risk LRP segment

In the non-culprit segment, 36 (19.8%) patients had at least one high-risk LRP segment, defined as a maxLCBI$_{4mm}$ ≥ 400. Lipid profiles such as LDL-C, non-HDL-C, MDA-LDL, and Lp(a) were similar between patients with at least one high-risk LRP segment and patients with no high-risk LRP segments (all p > 0.05). Similarly, in terms of inflammatory markers such as hs-CRP, TNF-α, and IL-6, there was no significant difference between patients with at least one high-risk LRP segment and patients with no high-risk LRP segments (all p > 0.05) (Supplemental Table 1).

We performed a univariable logistic regression analysis to evaluate predictors of non-culprit high-risk LRP. Age, male sex, and classical coronary risk factors such as hypertension, diabetes, and CKD did not predict high-risk LRP, whereas only plaque burden at the MLA and maximum attenuation angle predicted high-risk LRP. After adjustment for clinically important variables, independent predictors of high-risk LRP in non-culprit segments were plaque burden at the MLA (OR 1.52, 95%CI 1.01–2.39, p = 0.040) and the maximum attenuation angle (OR 1.14, 95%CI 1.08–1.22, p < 0.001) (Supplemental Table 2).

Table 2
Angiographical, IVUS and NIRS findings.

	Culprit segment				Non-culprit segment			
	Overall (n = 239)	ACS (n = 82)	SA (n = 157)	*p*	Overall (n = 202)	ACS (n = 69)	SA (n = 133)	*p*
Culprit vessel				0.37				0.50
LAD, n (%)	104 (43.8)	29 (35.8)	75 (48.0))		90 (44.5)	26 (37.6)	64 (48.1)	
RCA, n (%)	88 (37.1)	33 (40.7)	55 (35.2)		76 (37.6)	28 (40.5)	48 (36.0)	
LCX, n (%)	37 (15.6)	16 (19.7)	21 (13.4)		34 (16.8)	14 (20.2)	20 (15.0)	
LMT, n (%)	4 (1.6)	2 (2.4)	2 (1.2)		2 (0.9)	1 (1.4)	1 (0.7)	
IVUS findings								
Quantitative parameters								
Segment length, median [IQR] (mm)	23.4 [17.7, 31.0]	25.3 [18.0, 32.9]	23.0 [17.3, 29.9]	0.14	27.7 [17.7, 40.8]	28.2 [17.9, 42.6]	26.9 [17.6, 40.8]	0.66
MLA, median [IQR] mm^2	2.2 [1.7, 2.6]	2.1 [1.5–2.6]	2.2 [1.7, 2.6]	0.48	6.9 [4.4, 9.7]	7.4 [4.9, 10.2]	6.7 [4.3, 9.3]	0.31
Plaque burden at MLA, median [IQR] (%)	81 [76, 86]	84 [78, 88]	81 [75, 84]	0.002	52 [39, 62]	52 [38, 61]	52 [39, 63]	0.76
Qualitive assessment and parameters								
Culprit plaque type				<0.001				0.80
Soft, n (%)	103 (43.2)	49 (60.4)	54 (34.3)		28 (17.6)	10 (18.1)	18 (17.3)	
Fibrous, n (%)	53 (22.2)	11 (13.5)	42 (26.7)		68 (42.7)	26 (47.2)	42 (40.3)	
Calcific, n (%)	24 (10.0)	2 (2.4)	22 (14.0)		19 (11.9)	6 (10.9)	13 (12.5)	
Mixed, n (%)	58 (24.3)	19 (23.4)	39 (24.8)		44 (27.6)	13 (23.6)	31 (29.8)	
Maximum attenuation angle, median [IQR] (degree)	150 [65, 230]	200 [140, 278]	120 [0, 190]	<0.001	0 [0, 130]	45 [0, 132]	0 [0, 126]	0.30
Maximum attenuation angle ≥ 180°, n (%)	98 (41.8)	48 (60.0)	50 (32.4)	<0.001	18 (11.6)	6 (11.3)	12 (11.7)	0.93
Maximum calcium angle, median [IQR] (degree)	105 [45, 180]	97 [41, 173]	105 [50, 180]	0.38	80 [25, 135]	70 [17, 137]	85 [35, 135]	0.47
Maximum calcium angle ≥ 180°, n (%)	65 (26.3)	19 (23.7)	43 (27.7)	0.50	20 [12.9]	5 (9.6)	15 (14.5)	0.37
NIRS findings								
$MaxLCBI_{4mm}$, median [IQR]	413 [20., 585]	533 [385, 745]	361 [174, 527]	<0.001	207 [46, 347]	246 [52, 342]	185 [37, 350]	0.48
Lesion LCBI, median [IQR]	142 [56, 245]	191 [111, 270]	119 [43, 222]	<0.001	57 [8, 113]	58 [11, 119]	57 [7, 112]	0.74

ACS, acute coronary syndrome; CCS, chronic coronary syndrome; LAD, left anterior descending artery; RCA, right coronary artery; LCX, left circumflex artery; LMT, left main trunk; IVUS, intravascular ultrasound; MLA, minimum lumen area; LCBI, lipid core burden index.

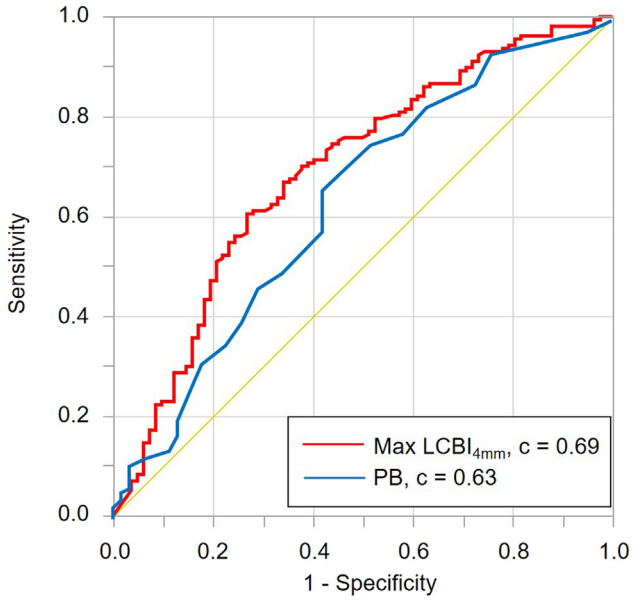

Fig. 2. Receiver-operating characteristic curve for the discrimination of ACS culprit segments by NIRS and IVUS. $MaxLCBI_{4mm}$ by NIRS, and PB at MLA by IVUS significantly discriminate ACS culprit from SA culprit lesion ($p < 0.001$, $p = 0.001$, respectively). ACS, acute coronary syndrome; NIRS, near infrared spectroscopy; IVUS, intravascular ultrasound; LCBI, lipid core burden index; PB, plaque burden; MLA, minimum lumen area; SA, stable angina pectoris.

4. Discussion

The major findings of this study were: (1) compared with SA culprit lesions, ACS culprit lesions had a higher $maxLCBI_{4mm}$, which substantiates that the $maxLCBI_{4mm}$ threshold to predict ACS was ≥ 400 in the Japanese population; (2) Almost 20% of patients had at least one high-risk LRP, defined as $maxLCBI_{4mm} \geq 400$ without a small lumen and with a large plaque burden in the non-culprit segments; (3) In overall study population, there was no significant association between NIRS $maxLCBI_{4mm}$ and circulating lipid profiles and inflammatory markers in both the culprit and non-culprit lesion segments; (4) the IVUS plaque burden and maximum attenuation angle were significantly associated with high-risk LRP in non-culprit segments.

Table 3
Multivariate Logistic Regression Analysis for Predicting ACS Culprit Lesion.

	Odds Ratio|	95% CI	*p*
Max $LCBI_{4mm} \geq 400$	3.87	1.95–8.02	<0.001
Plaque burden at MLA, 10% increase	1.58	0.99–2.60	0.06
Chronic kidney disease	1.88	0.85–4.17	0.11
Diabetes mellitus	0.64	0.32–1.27	0.20

ACS indicates acute coronary syndrome; CI, confidence interval; LCBI, lipid core burden index; MLA, minimum lumen area.

4.1. NIRS-derived LRP and IVUS lesion morphology in ACS culprit lesion

The present study demonstrates the potential clinical utility of intravascular imaging for diagnosing the ACS culprit lesion. Histological validation studies revealed the efficacy of IVUS imaging and the advantage of these modalities in assessing plaque burden and morphology [16,17]. Hong et al. revealed that the culprit lesion in patients with ACS are typically composed of a lipid core plaque [18]. Inaba et al. reported that a plaque burden ≥ 69% by IVUS and

a maxLCBI$_{4mm}$ ≥ 323 by NIRS predicted histopathological thin-cap fibroatheroma [19]. In the PROSPECT (Providing Regional Observations to Study Predictors of Events in Coronary Tree) study, an MLA < 4 mm^2 and a plaque burden ≥ 70% were predictors of subsequent lesion-related major adverse coronary events [20]. The efficacy of IVUS was limited due to limitations in the modality to detect plaque composition and the presence of lipids [21].

In the present study, no significant difference in MLA was observed between the ACS and SA culprit lesions. However, we confirmed that the maxLCBI$_{4mm}$ could better identify the ACS culprit segments than the plaque burden, and that an maxLCBI$_{4mm}$ ≥ 400 by NIRS could identify ACS culprit lesions with a relatively high specificity in the Asian population. Our current study showed that the maxLCBI$_{4mm}$ threshold may be similar regardless of ethnicity, and the validity of using an maxLCBI$_{4mm}$ of 400 as a cut-off can be assessed in future prospective studies in the Asian population. We also demonstrated that plaque burden at the MLA by IVUS indicated the presence of LRP by NIRS.

4.2. Relationship with NIRS derived maxLCBI$_{4mm}$ and clinical factors

MaxLCBI$_{4mm}$ by NIRS has been demonstrated to be associated with plaque vulnerability and adverse coronary events; however, whether surrogate markers such as lipid profiles and inflammatory markers predict LCBI has not been well investigated. Inflammation plays a central role in atherogenesis, from plaque formation to rupture [22,23]. We investigated the association of LCBI with patient coronary risk factors, lipids, and inflammatory markers that were reported to be associated with coronary events. However, no significant correlation was found between LCBI and systemic factors as lipids and inflammatory predictors, which were reported to be associated with plaque vulnerability. MDA-LDL is an oxidized LDL, which was shown to be elevated in patients with ACS [24]. Fujihara et al. reported that circulating MDA-LDL was associated with coronary stenosis in type 2 diabetes [25]. In our study, MDA-LDL levels showed a weak correlation with the maxLCBI$_{4mm}$ in patients with diabetes. Future large-scale studies are warranted to determine whether circulating biomarkers would be useful as a diagnostic marker for "vulnerable" patients with high-risk LRP by NIRS.

4.3. Predictors for the high risk LRP in non-culprit segments

Determining the plaque vulnerability of non-culprit segments is becoming increasingly important for predicting adverse cardiac events. The LRP (Lipid Rich Plaque) study revealed that the rates of non-culprit- and culprit-related major adverse cardiovascular events were similar, that 9% patients had subsequent non-culprit-related events within two years, and that LRP was an independent predictor for lesion-related cardiac events [7]. The current study surveyed systemic factors previously reported in vulnerable patients, and no predictors were found to be associated with the presence of LRP in non-culprit segments. In our study, only plaque burden at the MLA and the maximum attenuation angle by IVUS measurements in the non-culprit segment were significantly associated with non-culprit high-risk LRP. Despite significant advances in diagnostics from blood testing, identification of patients at a higher risk of future coronary events remains limited. We therefore believe that plaque evaluation by an invasive approach still remains an important element for the identification of high-risk LRP.

4.4. The rational for identification of plaque characteristics

The significance of identifying vulnerable plaques has not yet been established. It had been reported that the most of high-risk vulnerable plaques such as lipid-rich plaque remained quiescent and the positive predictive value of coronary imaging remained relatively low for clinical relevance [20,26,27]. On the other hand, optimal medical therapy such as lipid-lowering therapy has been established to decrease adverse clinical events in both primary and secondary prevention. However, it remains unclear for which patients and for how long costly drugs, including proprotein convertase subtilisin/kexin type 9 (PCSK9) inhibitor, should be used.

Detection of vulnerable plaques may help in patient stratification and in guiding pharmacotherapy (its intensity and duration). Identification of vulnerable plaque may facilitate optimal assignment of more aggressive and costly treatment strategies such as PCSK9 inhibitor and anti-inflammatory agents. In addition, PROSPECT ABSORB study (Providing Regional Observations to Study Predictors of Events in the Coronary Tree Ⅱ Combined with a Randomized, Controlled, Intervention Trial) demonstrated PCI for vulnerable plaque with angiographically mild stenotic lesion was associated with favorable long-term clinical outcomes [28].

This study revealed the characteristics of lipid rich plaque in Japanese patients with acute coronary syndrome and stable angina who has fewer adverse cardiovascular events than Caucasians. It is necessary to investigate whether more aggressive lipid-lowering therapy using PCSK9 inhibitor, anti-inflammatory therapy, and revascularization to vulnerable plaques are effective for East Asians.

4.5. Limitations

The present study has several limitations. First, because the sample size was relatively small and this was a single-center study, unknown confounding factors might have affected outcomes. Second, because NIRS-IVUS imaging was performed after aspiration thrombectomy (n = 26, 10.8%) if a thrombus was suspected from angiography, and/or balloon angioplasty (2.0 mm or less) (n = 33, 13.0%), if thrombolysis in myocardial infarction flow grade of 3 is not obtained, it may affect the measured IVUS parameters and LCBI. Third, stented segment which is definition of culprit lesion in current study might be affected and longer by operator's discretion who knew the result of NIRS-IVUS chemogram.

5. Conclusions

We confirmed that NIRS-IVUS plaque assessment could be useful to differentiate ACS from SA culprit lesions, and that a threshold maxLCBI$_{4mm}$ ≥ 400 was clinically suitable in Japanese patients. Further larger studies are needed to confirm the findings in Asian population. No systemic surrogate markers were found to be associated with the extent of LRP by NIRS in culprit and non-culprit segments. Consequently, we believe that direct intravascular evaluation of coronary plaque characteristics remains important for identification of high-risk LRP.

Ethics approval

The internal review board of the Juntendo University Hospital approved this study.

Consent to participate and for publication

Written informed consent to participate was obtained from all patients.

Availability of data and material

The data that support the findings of this study are available from the corresponding author, upon reasonable request.

Code availability

The relevant SAS codes for the statistical analysis are available from the corresponding author, upon reasonable request.

Financial support

This research received no external funding.

Author contributions

N Takahashi, T Dohi and H Endo analyzed data and wrote the manuscript under the supervision of K Miyauchi, H Iwata and T Minamino performed or supervised clinical data collection and phenotyping. M Takeuchi, S Doi, Y Kato, I Okai, S Okazaki and K Isoda provided technical and clinical contributions as well as discussion. All authors critically revised the manuscript and contributed substantially to this work. All authors have read and agreed to the manuscript.

Funding

Not applicable.

Declaration of Competing Interest

The authors declare that they have no known competing financial interests or personal relationships that could have appeared to influence the work reported in this paper.

Appendix A. Supplementary material

Supplementary data to this article can be found online at https://doi.org/10.1016/j.ijcha.2021.100747.

References

[1] J.E. Muller, G.H. Tofler, P.H. Stone, Circadian variation and triggers of onset of acute cardiovascular disease, Circulation 79 (1989) 733–743.
[2] E. Falk, M. Nakano, J.F. Bentzon, A.V. Finn, R. Virmani, Update on acute coronary syndromes: the pathologists' view, Eur. Heart J. 34 (2013) 719–728.
[3] R. Virmani, A.P. Burke, A. Farb, F.D. Kolodgie, Pathology of the vulnerable plaque, J. Am. Coll. Cardiol. 47 (2006) C13–C18.
[4] C.M. Gardner, H. Tan, E.L. Hull, J.B. Lisauskas, S.T. Sum, T.M. Meese, et al., Detection of lipid core coronary plaques in autopsy specimens with a novel catheter-based near-infrared spectroscopy system, JACC Cardiovasc. Imaging 1 (2008) 638–648.
[5] P.R. Moreno, R.A. Lodder, K.R. Purushothaman, W.E. Charash, W.N. O'Connor, J. E. Muller, Detection of lipid pool, thin fibrous cap, and inflammatory cells in human aortic atherosclerotic plaques by near-infrared spectroscopy, Circulation 105 (2002) 923–927.
[6] J.E. Muller, G.S. Abela, R.W. Nesto, G.H. Tofler, Triggers, acute risk factors and vulnerable plaques: the lexicon of a new frontier, J. Am. Coll. Cardiol. 23 (1994) 809–813.
[7] R. Waksman, C. Di Mario, R. Torguson, Z.A. Ali, V. Singh, W.H. Skinner, et al., Identification of patients and plaques vulnerable to future coronary events with near-infrared spectroscopy intravascular ultrasound imaging: a prospective, cohort study, The Lancet. 394 (2019) 1629–1637.
[8] R.D. Madder, M. Husaini, A.T. Davis, S. VanOosterhout, M. Khan, D. Wohns, et al., Large lipid-rich coronary plaques detected by near-infrared spectroscopy at non-stented sites in the target artery identify patients likely to experience future major adverse cardiovascular events, Eur. Heart J. Cardiovasc. Imaging 17 (2016) 393–399.
[9] R.D. Madder, R. Puri, J.E. Muller, J. Harnek, M. Götberg, S. VanOosterhout, et al., Confirmation of the intracoronary near-infrared spectroscopy threshold of lipid-rich plaques that underlie ST-segment-elevation myocardial infarction, Arterioscler. Thromb. Vasc. Biol. 36 (2016) 1010–1015.
[10] H. Ueshima, A. Sekikawa, K. Miura, T.C. Turin, N. Takashima, Y. Kita, et al., Cardiovascular disease and risk factors in Asia, Circulation 118 (2008) 2702–2709.
[11] K. Thygesen, J.S. Alpert, A.S. Jaffe, B.R. Chaitman, J.J. Bax, D.A. Morrow, et al., Fourth universal definition of myocardial infarction (2018), Eur. Heart J. 40 (2018) 237–269.
[12] G.S. Mintz, S.E. Nissen, W.D. Anderson, S.R. Bailey, R. Erbel, P.J. Fitzgerald, et al., American College of Cardiology clinical expert consensus document on standards for acquisition, measurement and reporting of intravascular ultrasound studies (ivus)31When citing this document, the American College of Cardiology would appreciate the follow, J. Am. Coll. Cardiol. 37 (2001) 1478–1492.
[13] Y. Saito, Y. Kobayashi, K. Fujii, S. Sonoda, K. Tsujita, K. Hibi, et al., Clinical expert consensus document on standards for measurements and assessment of intravascular ultrasound from the Japanese Association of Cardiovascular Intervention and Therapeutics, Cardiovasc. Interv. Ther. 35 (2020) 1–12.
[14] S. Waxman, S.R. Dixon, P. L'Allier, J.W. Moses, J.L. Petersen, D. Cutlip, et al., In vivo validation of a catheter-based near-infrared spectroscopy system for detection of lipid core coronary plaques: initial results of the SPECTACL study, JACC Cardiovasc. Imaging. 2 (2009) 858–868.
[15] R.D. Madder, J.A. Goldstein, S.P. Madden, R. Puri, K. Wolski, M. Hendricks, et al., Detection by near-infrared spectroscopy of large lipid core plaques at culprit sites in patients with acute ST-segment elevation myocardial infarction, JACC Cardiovasc. Interv. 6 (2013) 838–846.
[16] B.N. Potkin, A.L. Bartorelli, J.M. Gessert, R.F. Neville, Y. Almagor, W.C. Roberts, et al., Coronary artery imaging with intravascular high-frequency ultrasound, Circulation 81 (1990) 1575–1585.
[17] J. Pu, G.S. Mintz, S. Biro, J.B. Lee, S.T. Sum, S.P. Madden, et al., Insights into echo-attenuated plaques, echolucent plaques, and plaques with spotty calcification: novel findings from comparisons among intravascular ultrasound, near-infrared spectroscopy, and pathological histology in 2,294 human coronary artery segments, J. Am. Coll. Cardiol. 63 (2014) 2220–2233.
[18] M.K. Hong, G.S. Mintz, C.W. Lee, Y.H. Kim, S.W. Lee, J.M. Song, et al., Comparison of coronary plaque rupture between stable angina and acute myocardial infarction: a three-vessel intravascular ultrasound study in 235 patients, Circulation 110 (2004) 928–933.
[19] S. Inaba, G.S. Mintz, A.P. Burke, G.W. Stone, R. Virmani, M. Matsumura, et al., Intravascular ultrasound and near-infrared spectroscopic characterization of thin-cap fibroatheroma, Am. J. Cardiol. 119 (2017) 372–378.
[20] G.W. Stone, A. Maehara, A.J. Lansky, B. de Bruyne, E. Cristea, G.S. Mintz, et al., A prospective natural-history study of coronary atherosclerosis, N. Engl. J. Med. 364 (2011) 226–235.
[21] J. Pu, G.S. Mintz, E.S. Brilakis, S. Banerjee, A.R.R. Abdel-Karim, B. Maini, et al., In vivo characterization of coronary plaques: novel findings from comparing greyscale and virtual histology intravascular ultrasound and near-infrared spectroscopy, Eur. Heart J. 33 (2012) 372–383.
[22] K. Ikeda, Y. Souma, Y. Akakabe, Y. Kitamura, K. Matsuo, Y. Shimoda, et al., Macrophages play a unique role in the plaque calcification by enhancing the osteogenic signals exerted by vascular smooth muscle cells, Biochem. Biophys. Res. Commun. 425 (2012) 39–44.
[23] G.K. Hansson, Inflammation, atherosclerosis, and coronary artery disease, N. Engl. J. Med. 352 (2005) 1685–1695.
[24] P. Holvoet, J. Vanhaecke, S. Janssens, F. Van De Werf, D.S. Collen, Oxidized LDL and malondialdehyde-modified LDL in patients with acute coronary syndromes and stable coronary artery disease, Circulation 98 (1998) 1487–1494.
[25] K. Fujihara, H. Suzuki, A. Sato, S. Kodama, Y. Heianza, K. Saito, et al., Circulating malondialdehyde-modified LDL-related variables and coronary artery stenosis in asymptomatic patients with type 2 diabetes. J. Diabetes Res. 2015; 2015: 507245-.
[26] S. de Boer, Y. Baran, H.M. Garcia-Garcia, I. Eskin, M.J. Lenzen, M.E. Kleber, et al., The European collaborative project on inflammation and vascular wall remodeling in atherosclerosis - intravascular ultrasound (ATHEROREMO-IVUS) study, EuroIntervention 14 (2018) 194–203.
[27] P.H. Stone, S. Saito, S. Takahashi, Y. Makita, S. Nakamura, T. Kawasaki, et al., Prediction of progression of coronary artery disease and clinical outcomes using vascular profiling of endothelial shear stress and arterial plaque characteristics: the PREDICTION Study, Circulation 126 (2012) 172–181.
[28] G.W. Stone, A. Maehara, Z.A. Ali, C. Held, M. Matsumura, L. Kjøller-Hansen, et al., Percutaneous coronary intervention for vulnerable coronary atherosclerotic plaque, J. Am. Coll. Cardiol. 76 (2020) 2289–2301.